

https://doi.org/10.1093/femsec/fiab118

Advance Access Publication Date: 19 August 2021 Research Article

RESEARCH ARTICLE

Microbially mediated nitrogen removal and retention in the York River Estuary

Samantha G. Fortin*,†, Bongkeun Song and Iris C. Anderson

Virginia Institute of Marine Science, William & Mary, Gloucester Point, VA 23062, USA

*Corresponding author: PO Box 1346, Gloucester Point, VA 23062, USA. Tel: (804)684-7411; E-mail: sgfortin@vims.edu

One sentence summary: Determining geochemical and microbial controls on benthic nitrogen cycling processes in the York River Estuary.

Editor: Lee Kerkhof

†Samantha G. Fortin, https://orcid.org/0000-0002-0062-963X

ABSTRACT

Denitrification, anaerobic ammonium oxidation and dissimilatory nitrate reduction to ammonium (DNRA) are important microbial processes determining the fate of nitrogen (N) in estuaries. This study examined these processes in sediments of the York River Estuary, a tributary of Chesapeake Bay, and investigated environmental and microbial drivers of the rates of denitrification and DNRA. Nitrate reduction followed a consistent pattern throughout the year and across the estuary with nitrogen removal, primarily through denitrification, decreasing from the head of the estuary to the mouth and nitrogen retention, through DNRA, following the opposite pattern. At the mouth of the estuary, nitrogen retention was consistently higher than nitrogen removal. Denitrification rates showed strong linear relationships with concentrations of organic matter, nitrate and chlorophyll a, and the abundance of the nirS gene. DNRA rates were best correlated with the relative abundance of three bacterial families, Anaerolineaceae, Ectothiorhodospiraceae and Prolixibacteraceae, which carry the nrfA gene. The controls responsible for retention or removal of N from an estuary are complex, involving both geochemical and microbial factors. The N retained within estuaries may support primary production and seasonal algae blooms and result in estuarine eutrophication.

Keywords: denitrification; anammox; DNRA; nitrate reduction; microbial communities

INTRODUCTION

Estuaries are important ecosystems where freshwater, transporting terrestrially derived nutrients and organic matter, mixes with seawater. Estuaries typically display large salinity gradients, varying with freshwater discharge, with fresher water at the head and brackish water at the mouth. The terrestrially derived nutrients entering the estuarine system are used by numerous autotrophic and heterotrophic microorganisms throughout the estuary, creating geochemical gradients of salinity, carbon (C), nitrogen (N) and other nutrients. These gradients lead to shifts in the community structure of phytoplankton, bacteria and other microbial organisms along the estuarine continuum (Schultz and Ducklow 2000). Furthermore, C and nutrient cycling in estuaries can play an important role

in determining what concentrations and types of nutrients are exported to coastal and open ocean ecosystems.

Estuaries are often hotspots for N cycling processes, especially as growing human populations in coastal areas intensify anthropogenic impacts and lead to greater nutrient additions to estuarine systems (Kemp et al. 2005). These watershed-delivered nutrients, along with autochthonous and allochthonous organic matter, are processed throughout estuaries. In particular, the nitrate (NO3 $^-$) delivered to the estuary through run-off and point sources is consumed by benthic microbes in one of three processes. Denitrification, the reduction of fixed nitrogen such as NO3 $^-$ and nitrite (NO2 $^-$) to gaseous N including nitric oxide (NO), nitrous oxide (N2O) and dinitrogen gas (N2), is the major nitrogen removal pathway mediated by benthic microbial communities. Anammox (anaerobic ammonium oxidation), the

oxidation of ammonium (NH_4^+) coupled to the reduction of NO_2^- to N_2 , is another N removal pathway present in estuarine sediments, generally accounting for 10–20% of the N_2 production in estuaries (Rich *et al.* 2008). Dissimilatory nitrate reduction to ammonium (DNRA), which reduces NO_3^- to NH_4^+ , retains N within the ecosystem. These competing NO_3^- reduction processes are mediated by specific prokaryotic functional groups that are influenced by the geochemical conditions of the benthic environment (Dong *et al.* 2009; Song, Lisa and Tobias 2014).

Geochemical controls on denitrification, anammox and DNRA have been explored in a number of estuaries and other coastal ecosystems. DNRA is favored over denitrification in ecosystems with high organic carbon (OC) to NO₃⁻ ratios (Song, Lisa and Tobias 2014; Hardison et al. 2015) and high levels of sulfate reduction and sulfide oxidation (Bohlen et al. 2011; Giblin et al. 2013), as well as when temperatures are high (Giblin et al. 2013). Salinity has also been found to be a large factor, negatively affecting rates of denitrification and positively correlating with DNRA (Giblin et al. 2010, 2013). Furthermore, salinity has been found to be a driver of microbial community structure for those microbes performing DNRA (Song, Lisa and Tobias 2014). However, understanding regarding the relative importance of these N removal and retention processes across estuarine gradients is limited by the small number of studies examining DNRA and its controlling factors in estuarine systems (Giblin et al. 2013).

This study investigates the microbial and geochemical controls on benthic N cycling in a temperate, microtidal, river-driven estuary that receives large inputs of N and dissolved organic C. Specifically, this study examines changes in the rates of denitrification, anammox and DNRA over spatial and temporal scales while determining biotic and abiotic drivers. Furthermore, specific microbial taxa associated with N cycling processes are identified to better understand the conditions and locations in which N retention outpaces N removal in estuarine sediments.

METHODS

Sampling

The York River is the fifth largest tributary to Chesapeake Bay and receives water from the Mattaponi and Pamunkey Rivers. Nutrient loading is dominated by forested and agricultural runoff (61% and 21% land cover of the watershed, respectively) that is delivered to the estuary through river flow (Reay 2009). Wastewater treatment plants, both residential and industrial, make up a smaller proportion of nutrient loading (Reay 2009). This results in a geochemical gradient in which the head of the estuary has the lowest salinity and, generally, the highest NO₃concentrations, while the mouth of the estuary has the highest salinity (Reay 2009). The major estuarine turbidity maximum is located at the head of the estuary, though a second turbidity maximum can occur seasonally in the upper or mid portion of the estuary (Lin and Kuo 2001). Harmful algal blooms and hypoxia are common in the lower portion of the estuary in the summer months (Reay 2009; Marshall and Egerton 2012).

Sampling took place at five stations (Fig. 1), 1 m in depth (mean sea level) along the length of the York River in June, August and October 2018, and February and April 2019. At each station, a YSI took measurements of water column temperature, salinity, chlorophyll *a*, turbidity and dissolved oxygen at a depth of 0.5 m. Further water column data, including nutrient concentrations, were obtained from samples taken at the same stations the previous day. All dissolved (0.45 µm filtered) inorganic N (DIN) in the water column was analyzed using a

Lachat QuikChem FIA+ 8000 (Hach, Loveland, CO, USA) in duplicate (detection limits: 0.2 µM nitrate and nitrite, 0.36 µM ammonium). Two sediment cores (5.6 cm diameter, 10 cm deep) were collected at each station and transported to the Virginia Institute of Marine Science (VIMS) where the top 2 cm were separated from the rest of the core for further analysis. The top 2 cm from both replicate cores were composited, split into two 50-mL tubes, centrifuged and the resulting pore water was frozen for nutrient analysis as described above. One of the 50 mL tubes of composited sediment was stored for one day at 5°C for nitrogen cycling rate analysis; the other was frozen at -80°C for molecular and % organics analyses. The frozen sediment was freezedried, homogenized and analyzed with an elemental analyzer (Model 1040, Costech, Valencia, CA, USA) attached to an isotope ratio mass spectrometer (IRMS, Model Delta V, ThermoScientific, Waltham, MA, USA) for determination of total carbon and nitrogen content.

Slurry incubation experiments

One gram of sediment from each composited sample was weighed into five Exetainer tubes (Labco, Lampeter, UK). After flushing for 5 min with helium (He) gas to create anoxic conditions, the tubes were incubated at in situ temperatures overnight to remove all background nitrate and re-flushed with He gas. One tube for each sample was frozen for analysis to check that all background NO_3^-/NO_2^- was removed by the overnight incubation. The remaining four tubes were used, in duplicate, as the initial time point (To) and the final time point (TF) for the potential rate measurement incubations.

Denitrification and anammox potential rate measurements were performed following established protocols (Song and Tobias 2011; Semedo and Song 2020); DNRA potential rate measurements followed a modified protocol from Yin *et al.* (2014). Each gram of sediment was spiked with 100 nmol of ¹⁵NO₃⁻ (99 atom%, Cambridge Isotopes, Tewksbury, MA, USA) and incubated at in situ temperatures. The addition of 50% zinc chloride (0.5 mL) was used to stop all microbial activity immediately after spiking with ¹⁵NO₃⁻, for T₀, or after a 1-h incubation, for TF. The amount of accumulated ³⁰N₂ and ²⁹N₂ was then measured in the gas fraction using an IRMS. Immediately following IRMS analysis, the Exetainers were frozen until analyzed for DNRA.

Ammonium was extracted from the sediment incubation samples using 5 mL of 2 M potassium chloride (KCl). For each sample, 4 mL of the KCl extract were diluted with 22 mL of autoclaved, Milli-Q (MilliporeSigma, Burlington, MA, USA) filtered water and poured into two new Exetainer tubes. One tube was left as a control and run on a membrane inlet mass spectrometer (MIMS, Balzers Prisma, Pfeiffer, Aßlar, Germany) without any further additions; the second tube was spiked with 200 μL of a hypobromite solution that converts all NH₄+ to N₂ (Yin et al. 2014), inverted and incubated for at least 15 min before being run on the MIMS. The concentration of excess 29 N2 and 30 N2 produced by the addition of the hypobromite solution was calculated for each sample based on the method of Risgaard-Petersen and Rysgaard (1995) with the exception that a single air equilibrated DI water standard, held at the same temperature as the samples, was used. The concentrations of excess ²⁹N₂ and ³⁰N₂ were used to calculate the concentration of ¹⁵NH₄⁺ present in

Rates of denitrification and anammox were calculated from the amount of $^{30}N_2$ and $^{29}N_2$, respectively, produced between T_0 and TF (1 h) in each of the duplicate analytical replicates and DNRA rates were calculated based on the concentrations of

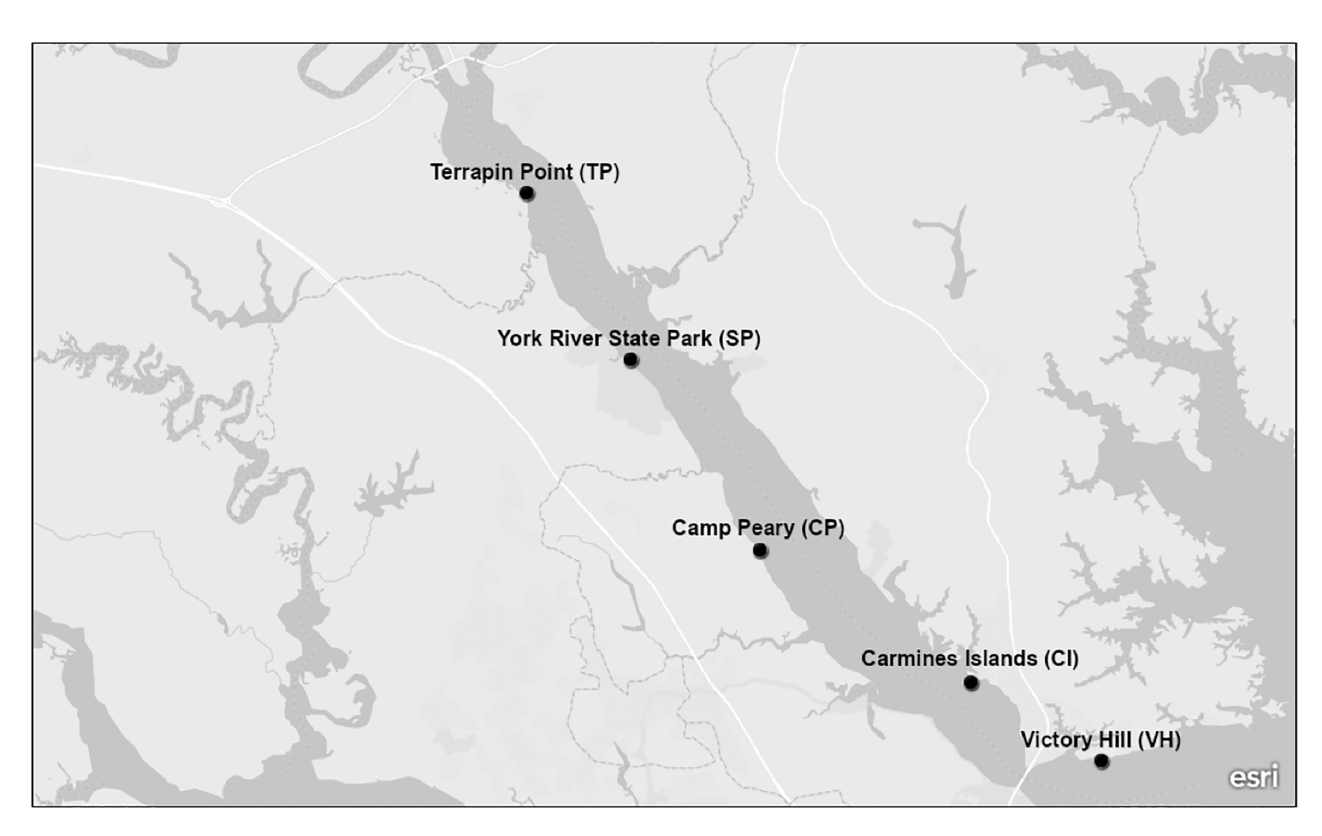


Figure 1. A map of the York River Estuary, VA, USA. Stations are represented by black dots and range the length of the York River Estuary from the head (Head Estuary Shoal) to the mouth (Mouth Estuary Shoal). All stations were located on the shoal of the estuary (1 m in depth).

 $^{15}\mathrm{NH_4}^+$ produced between T₀ and TF (1 h) in each of the duplicate analytical replicates (Fig. S1, Supporting Information). Since DNRA, denitrification and anammox took place simultaneously in the vials, the ¹⁵NH₄⁺ produced by DNRA could have been used by anammox bacteria in combination with the ¹⁵NO₃⁻ to produce ³⁰N₂, leading to a potential overestimation of denitrification rates and underestimation of anammox rates. To account for this, the anammox and denitrification rates were corrected based on equations found in Salk et al. (2017). The concentration of ³⁰N₂ produced by anammox was calculated as

$$AMX_{30} = \frac{A_{29}}{r_{14a}},\tag{1}$$

where A_{29} is the concentration of $^{29}N_2$ measured on the IRMS and r_{14a} is the ratio of $^{14}NH_4+^{15}NH_4+^{15}$ found in the final time point of each DNRA sample. The AMX₃₀ calculation was determined for each sample individually and was added to or subtracted from the measured concentrations of ²⁹N₂ and ³⁰N₂, respectively at TF, when calculating rates of anammox and denitrification. The highest and lowest rates of denitrification, anammox and DNRA were extrapolated from nmoles g-1 h-1 to μmoles m⁻² h⁻¹ by multiplying them by the bulk density of the sediment, the thickness of the sediment layer (2 cm) homogenized for rate measurements and the conversion factor between centimeters and meters. Bulk density was measured at one time point by dividing the sediment dry weight by the sediment volume in the top 2 cm of sediment cores from each station.

Microbial community analysis

DNA was extracted from each composited sediment sample using 0.5 g of sediment and the DNeasy PowerSoil Kit (Qiagen,

Hilden, Germany) following the manufacturer's protocols. The abundance of specific genes was measured using SYBR Green quantitative PCR (qPCR). The DNRA marker gene nrfA was measured using the primers nrfA2F/nrfA1R (Mohan et al. 2004; Welsh et al. 2014) and the following qPCR reaction: 6 µL of GoTaq qPCR Master Mix (Promega, Madison, WI, USA), 0.03 µL of CXR Reference Dye (Promega, Madison, WI, USA), 0.6 µL of each primer, 0.25 μ L of MgCl₂ and 4 μ L of sample DNA (at 1 ng/ μ L) with the remainder of the 12 µL reaction volume made up with DNAasefree water. The nrfA qPCR protocol included an initial 10 min step at 95°C followed by 50 cycles of: 95°C for 15s, 52°C for 45 s, 72°C for 1 min and 80°C for 35 s (Song, Lisa and Tobias 2014). The qPCR reaction for nirS, the denitrification marker gene, included: 6 μL of GoTag qPCR Master Mix, 0.03 μL of CXR Reference Dye, 0.6 μL of the forward primer nirScdaF (Kandeler et al. 2006), 0.6 µL of the reverse primer nirSR3cd (Kandeler et al. 2006), 0.12 µL of BSA and $4 \mu L$ of sample DNA (at 1 ng/ μL) with the remainder of the 12 μL reaction volume made up DNAase-free with water; the protocol was: 95°C for 10 min, followed by 45 cycles of 95°C for 15 s, 57°C for 1 min, 72°C for 1 min and 80°C for 35 s. The 16S rRNA gene qPCR reactions were set up in the same way as the nirS reactions, with the exception that the primers 515F-Y (Parada, Needham and Fuhrman 2016) and 806R (Caporaso et al. 2011) were used. The 16S rRNA gene qPCR protocol is as follows: 95°C for 10 min with 40 cycles of 95°C for 15 s, 55°C for 30 s and 70°C for 30 s, with a melting curve analysis at the end. All qPCR samples were run in triplicate, with two no-template negative controls for each run. Gene abundance was calculated based on a standard curve produced with known quantities of the target gene (R2 values: 0.997, 0.996 and 0.993 for nrfA, nirS and 16S rRNA gene, respectively). Specificity of qPCR reactions was confirmed with melting curves, and efficiencies were calculated (48.95%, 107.67% and 79.68% for nrfA, nirS and 16S rRNA gene, respectively).

Microbial community composition was examined using Illumina (San Diego, CA, USA) sequencing of 16S rRNA genes amplified with 515F-Y (Parada, Needham and Fuhrman 2016) and 806R (Caporaso et al. 2011) and the following protocol: 95°C for 3 min, followed by 25 repetitions of 95°C for 30 s, 55°C for 1 min and 72°C for 1 min with a final elongation step of 72°C for 5 min. PCR took place in 25 µL reactions containing 12.5 µL of GoTaq Master Mix, 1 μ L of each primer, 515F-Y and 806R (10 mM) and 2 μ L of sample DNA (1 ng/µL concentration) with the rest of the volume made up with water. Amplified genes were then indexed with Nextera XT index primers (Illumina, San Diego, CA, USA) during a second PCR with the following protocol: 95°C for 3 min, followed by eight repetitions of 95°C for 30 s, 55°C for 30 s and 72°C for 30 s with a final elongation step of 72°C for 5 min. Following amplification, 16S rRNA genes were purified with Mag-Bind TotalPure NGS (Omega Bio-Tek, Norcross, GA, USA), following the manufacturer's protocols, before being sequenced on an Illumina MiSeq.

All bioinformatic processing and 16S rRNA gene sequence analysis was performed with R version 3.6.1 (R Core Team 2018). Sequences were processed using the DADA2 pipeline (Callahan et al. 2016). Trimmed sequences that passed the quality control and chimera checks were identified using the SILVA taxonomic database version 132 (Yilmaz et al. 2014). Further analysis was performed with phyloseq (McMurdie and Holmes 2013), and graphics were produced using ggplot2 (Wickham 2005). Specific amplicon sequence variants (ASVs) that appeared fewer than 10 times across all samples were removed. Sequences can be found in NCBI GenBank under BioProject PRJNA665972.

Extracted DNA from the October sediment samples representing spatial variation of sediment communities was sent to Novogene Co., Ltd (Beijing, China) for metagenomic sequencing using the Illumina platform. The resulting metagenomic sequences were uploaded to the KBase platform (Arkin et al. 2018) for analysis. The quality of the sequences were checked with FastQC (Andrews 2010) and sequences were trimmed with Trimmomatic (Bolger, Lohse and Usadel 2014). Sequence annotation, with a focus on nitrogen cycling genes, was performed with FamaProfiling (https://github.com/novichkov-lab/f ama). Taxa carrying nrfA and nirS were identified based on the FamaProfiling annotated sequences. Figures depicting community structure of nrfA and nirS carrying organisms based on metagenomic data were created using Phyloseq (McMurdie and Holmes 2013) and ggplot2 (Wickham 2005) based on the efpkg gene normalization calculated by FamaProfiling (https://github .com/novichkov-lab/fama).

Statistical analysis

All statistical analyses were performed with R version 3.6.1 (R Core Team 2018). One-way analysis of variance (ANOVA) tests were run on nitrogen cycling process rates and environmental variables. Due to lack of replicate samples for a season/station pair, ANOVAs were run to test either for temporal variation (combining all stations as replicates) or for spatial variation (combining all seasons as replicates). Pairwise t-tests with Bonferroni corrected P-values ($\alpha=0.05$) were used to compare multiple seasons and stations as appropriate. Normality was tested using Normal Q-Q and residual plots and variables were log transformed as necessary.

The factors impacting dissimilarity between entire microbial communities were tested using a permutational multivariate analysis of variance (PERMANOVA). A Bray-Curtis distance matrix of the microbial community samples was calculated

using phyloseq (McMurdie and Holmes 2013); the PERMANOVA test was performed with the adonis function in vegan (Oksanen et al. 2018) as was a test for the homogeneity of dispersion of the samples using the betadisper function. A canonical analysis of principal components (CAP) was used to identify environmental factors driving differences in microbial community structure using the same Bray–Curtis distance matrix used for the PERMANOVA test.

Multiple linear regressions were used to determine what environmental and molecular characteristics explained variations in denitrification and DNRA rates. All explanatory variables were checked for covariance using a variance inflation factor test. If covariance was found, single linear regressions were performed for the covarying variables; the one with a lower AICc was kept in the multiple linear regression. In the case of overlapping variables, for example water column versus pore water nutrients, variables with the better single linear regressions, based on the small-sample corrected Akaike information criterion (AICc), were selected for each modeled process. Normality was tested with Normal Q-Q and residual plots; where necessary variables were log transformed. The AICc and adjusted R2 of each possible multiple linear regression model were calculated using the Mu-MIn package (Barton 2009); only models with a delta AICc <2 were considered.

RESULTS

Geochemical characteristics of water and sediment

Water temperatures in the York River remained consistent throughout the estuary and followed typical seasonal trends for temperate estuaries with significantly higher temperatures in June, August and October 2018, and significantly lower temperatures in February and April 2019 (ANOVA, F = 4422.8, P < 0.05; Table 1). Salinity, which varied significantly across the estuary (F = 19.9, P < 0.05), was lowest in the upper portion of the estuary and increased steadily moving down estuary (Table 1). June 2018 had higher than average precipitation and fresh water discharge resulting in the lowest salinity observed during the course of the study in the upper portion of the estuary. Water column dissolved oxygen was significantly higher (F = 29.4, P < 0.05) in February and April 2019 than in June, August and October 2018 (Table 1). Water column DIN, both NO_x^- ($NO_3^- + NO_2^-$) and NH_4^+ , followed a similar spatial pattern, a decrease from the head of the estuary to the mouth, except during August in which NH₄+ increased in the Lower and Mouth estuary stations, though there were no significant spatial or temporal trends. DIN was higher, especially at the head of the estuary, during June 2018, likely due to the higher than average river flow, and was dominated by NO_x throughout most of the year (Table 1).

Sediment in the York River was muddy at the head and became sandier near the mouth of the estuary. The sediment % organic content was significantly higher in the upper portion of the estuary than in the lower portion (F = 19.3, P < 0.05); it rapidly decreased down estuary from the Upper Estuary station in February and April 2019 but exhibited a more gradual decrease during other sampling periods (Table 1). Sediment C:N was more varied and showed no significant spatial or temporal trends, though it was highest in the lower portion of the estuary in a majority of months (Table 1). Pore water $NO_{\rm X}$ concentrations remained fairly consistent throughout the estuary except for spikes at the Upper Estuary and Lower Estuary stations in February 2019, whereas pore water NH_4^+ , which was higher than

Downloaded from https://academic.oup.com/femsec/article/97/9/fiab118/6354774 by guest on 28 August 2021

Table 1. Environmental characteristics from the York River Estuary. Salinity, chlorophyll a (Chl a, µg/L), water column concentrations of ammonium (WC NH4, µM) and nitrate/nitrite (WC NO_x, µM),

processing.		•					'	,			•
Month	Station	Salinity	Chl a	WC NH4	WC NO _x	Temp	DO	% Organic	C:N	PW NH₄	PW NO _x
June	Head	3.03	8.10	18.42	61.21	23.96	4.47	16.91	10.96	44.82	0.56
August	Head	6.90	16.70	6.20	31.80	28.85	4.08	18.32	12.78	75.48	0.71
October	Head	6.43	17.00	1.77	23.32	25.02	4.74	18.51	11.86	39.97	0.44
February	Head	4.18	3.50	1.03	2.51	4.61	11.24	26.85	13.32	44.07	0.54
April	Head	5.28	4.60	8.77	16.68	12.07	8.37	17.14	12.80	67.12	0.52
June	Upper	6.23	9.80	7.22	20.67	24.09	4.93	12.60	16.68	45.03	0.62
August	Upper	9.88	14.30	3.00	29.19	29.31	4.52	13.66	11.33	40.53	0.56
October	Upper	9.59	32.30	1.22	11.48	25.61	5.88	13.45	11.76	50.68	0.68
February	Upper	7.00	3.80	0.64	0.01	5.14	11.32	0.85	16.00	8.00	16.70
April	Upper	6.41	10.90	8.91	16.29	12.45	8.97	1.45	11.11	22.58	2.07
June	Mid	8.77	13.10	2.78	38.79	23.79	6.72	1.97	9.80	83.94	0.80
August	Mid	13.33	13.60	0.60	24.61	29.46	4.97	5.35	8.71	89.43	0.56
October	Mid	12.11	12.30	0.72	8.46	35.38	6.11	8.00	10.33	76.69	0.64
February	Mid	8.55	4.40	0.50	0.03	5.60	12.57	0.99	11.00	14.22	06.0
April	Mid	8.70	49.50	5.18	12.18	12.32	11.03	1.46	10.83	39.35	1.13
June	Lower	12.04	00.9	2.01	30.28	24.19	5.38	0.40	7.50	90.39	2.18
August	Lower	14.72	15.10	1.14	23.76	29.08	6.55	0.51	15.00	12.95	1.01
October	Lower	14.12	9.00	0.30	10.68	25.80	6.48	0.94	22.00	35.38	1.20
February	Lower	11.01	13.40	0.44	0.05	5.73	14.09	0.36	6.50	51.20	16.36
April	Lower	11.56	27.90	0.09	1.59	11.70	10.79	0.32	8.50	27.43	1.76
June	Mouth	13.99	8.90	90.0	22.18	23.79	7.34	0.53	9.00	54.26	1.36
August	Mouth	16.35	8.00	2.23	28.72	29.53	8.21	0.78	6.33	69.69	1.63
October	Mouth	15.02	12.00	0.46	0.44	25.75	6.71	0.65	24.71	72.89	0.98
February	Mouth	12.63	15.40	0.42	0.08	5.76	14.50	0.85	21.83	105.12	2.45
April	Mouth	12.34	6.40	60.0	5.00	12.55	10.30	0.83	24.38	25.58	1.43

pore water NO_x-, varied widely across the estuary, though neither showed significant trends (Table 1).

Potential rate measurements of anammox, denitrification and DNRA

Potential denitrification rates ranged from 0.75 nmoles N per gram of sediment per hour (nmoles N g⁻¹ h⁻¹) to 75.75 nmoles N g $^{-1}$ h $^{-1}$ (Table 1) or 18.36 to 618.93 μ moles N m $^{-2}$ h $^{-1}$. Denitrification rates followed a consistent spatial pattern with the highest rates in the upper estuary and a sharp drop in rates down estuary from the Mid Estuary station. Mouth and Lower Estuary stations had consistently, and significantly (F = 7.0, P < 0.05), lower rates of denitrification than Head Estuary (Fig. 2). Overall, denitrification rates were highest in June and lowest in February, though there were no significant temporal trends (Table 2). Potential anammox rates were lower than denitrification rates and ranged from 0.03 to 6.62 nmoles N g-1 h-1 (0.74-54.13 μ moles N m⁻² h⁻¹); anammox followed the same spatial pattern as denitrification (Fig. 2) and was significantly lower at Lower and Mouth Estuary than Head and Upper Estuary (F = 7.9, P < 0.05). Anammox made up between 1.3% and 13.6% of total nitrogen removal (denitrification + anammox). Potential DNRA rates, which ranged from 0.11 to 15.15 nmoles N g⁻¹ h⁻¹ (0.90-368.87 µmoles N m⁻² h⁻¹), were consistently lowest at the Upper Estuary station and were significantly higher at Mouth Estuary when compared to any other station (F = 10.5, P < 0.05; Fig. 2). For October, February and April, the second highest DNRA rates were found at the Lower Estuary station (Table 2). Temporally, DNRA rates remained fairly consistent throughout June, August and October, and were lowest, though not significantly, in February (Table 2).

Microbial community composition and abundance of NO₃⁻ reducing communities

Sediment microbial communities were dominated by Proteobacteria (Delta and Gamma) and Bacteroidia regardless of month or station (Fig. 3). Oxyphotobacteria increased, whereas Anaerolinea decreased, in relative abundance down estuary. Alpha diversity, as measured by Shannon Index, remained consistent across the estuary each month, with the exception of the Mouth Estuary station in June 2018, which was lower than any other time point. Alpha diversity was significantly higher in the warmer months, June, August and October (2018), than in February 2019 (F = 8.3, P < 0.05; Table 2).

Beta diversity of the sediment microbial community was primarily driven by spatial separation (PERMANOVA, F = 3.7, P <0.05) (Fig. 4). The lower estuarine stations (Mouth and Lower) separated out from the upper estuarine stations (Mid, Upper, Head). Mid Estuary separated out slightly from Upper and Head Estuary, though to a lesser degree than the separation between the upper and lower estuarine stations. Beta diversity was also driven, to a lesser degree, by month (F = 2.9554, P < 0.05). For all stations, August and October grouped together as did February and April. June samples showed a slight separation from August and October for Mouth, Lower and Mid Estuary. June, August and October samples from Head and Upper Estuary clustered very closely together with a greater shift in the February and April samples for Upper Estuary than Head (Fig. 4).

Microbial community beta-diversity was not only driven by spatiotemporal variation but also by environmental factors. A canonical analysis of principle components (CAP) showed that water column salinity, water column temperature and sediment % organic matter were major drivers of sediment microbial communities in the York River (Fig. S2, Supporting Information). Salinity was a major driver of sediment communities in the lower portion of the estuary while sediment % organics was associated with the Head and Upper estuarine station communities (Fig. S2, Supporting Information). Temperature was associated with the warmer months of June, August and October. Water column concentrations of NO_x, NH₄ and chlorophyll a were less important drivers of sediment microbial community structure (Fig. S2, Supporting Information).

The abundance of nirS genes in the York River sediment ranged from 6.63×10^2 gene copies per gram of sediment (copies $g^{-1})$ to 3.46×10^6 copies g^{-1} with a significantly lower abundance of nirS genes in Lower and Mouth Estuary when compared to the Head Estuary station (ANOVA, F = 3.9, P < 0.05; Table 2). The abundance of nrfA genes ranged from 4.50 \times 10³ to 3.64 \times 10⁶ copies g-1 and showed no spatial patterns across the estuary (Table 2).

Organisms capable of carrying out denitrification or DNRA, based on the presence of nirS and nrfA, respectively, were identified using metagenomic sequencing for the October York River sediment samples. Since the York River sediment communities were primarily driven by spatial variation, rather than temporal, the October sediment communities were considered representative of all seasons. Based on identification of nirS genes in the October sediment metagenomes, the majority of denitrifiers in the York River were Proteobacteria, primarily Gammaproteobacteria (Fig. 5). The metagenome normalized number (efpkg) of nirS genes was lower in the Lower and Mouth Stations than in the upper portions of the estuary during October. Organisms carrying nrfA were dominated by Desulfuromonadales, especially in the upper portions of the estuary, Deltaproteobacteria and Gammaproteobacteria (Fig. 5). Similar to nirS, the normalized number of nrfA genes decreased at Lower and Mouth Estuary Stations in October even though DNRA rates were higher at those stations. The families carrying nrfA across all samples, based on 16S rRNA gene data, were dominated by Anaerolineaceae and Flavobacteriaceae (Fig. S3, Supporting Information).

Drivers of nitrogen cycling processes

Linear modeling was performed to determine the drivers of nitrogen removal and retention in the estuary, in the form of denitrification and DNRA rates, respectively; anammox was not modeled due to its low contribution to overall nitrogen removal. Sediment denitrification rates were best predicted by a combination of environmental factors and denitrification gene abundance. The top multiple linear regressions (delta AICc <2), which included seven different models that explained an average of 87% of the variation in denitrification rates, included the following variables: % sediment organic matter (seven of the top models), water column NO_x concentrations (seven), water column Chl a (four), nirS gene abundance (three) and water column salinity (three). The best model included only % sediment organic matter and water column NO_x- (Table S1, Supporting Information). Since denitrification rates were well predicted by the entire nirS carrying community, further efforts to determine the effects of individual nirS carrying taxa were not conducted. Sediment chlorophyll was not measured in June and, therefore, could not be included in the multiple linear regressions; based on single linear regressions, sediment chlorophyll was significantly, negatively correlated with denitrification rates (P < 0.05, $R^2 = 0.33$).

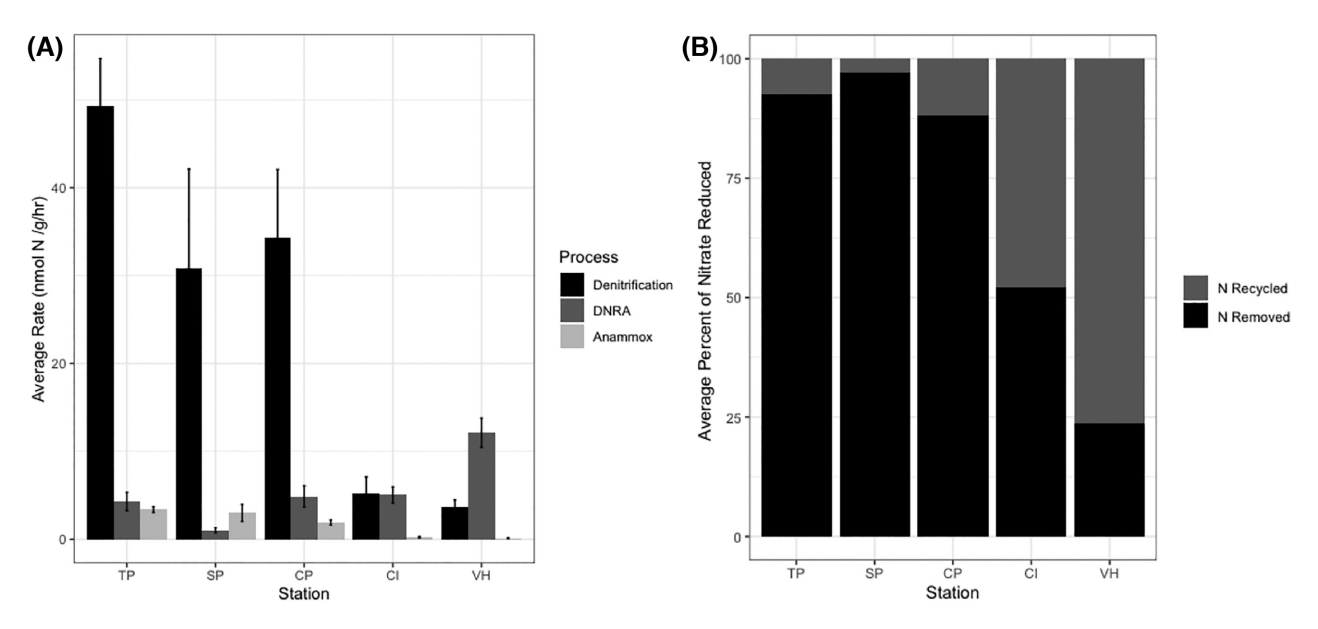


Figure 2. The yearly average of nitrogen removal and recycling processes across five stations in the York River Estuary ranging from the head of the estuary (Head) to the mouth (Mouth). (A) Average (of 5 months) rates of denitrification, DNRA and anammox (nmoles N $g^{-1} h^{-1}$). Error bars represent standard error. (B) Average (of 5 months) % of nitrate reduced by a nitrogen removal process (denitrification and anammox) or a nitrogen recycling process (DNRA) at each station.

Table 2. Rates of nitrate reduction processes across the York River Estuary from June 2018 to April 2019 and associated sediment microbial functional gene abundances as measured with qPCR. All nitrogen cycling process rates are in nmoles N g⁻¹ h⁻¹. DNF stands for denitrification; AMX stands for anammox. Rates are an average of two analytical replicates; gene copies are an average of three analytical replicates.

Month	Station	DNF	AMX	DNRA	nirS	nrfA	16S	Shannon Diversity Index
June	Head	67.38	3.68	8.79	3.46·10 ⁶	3.21·10 ⁶	3.41·10 ⁷	6.36
August	Head	57.94	3.07	3.85	$1.92 \cdot 10^{6}$	$1.44 \cdot 10^6$	$2.16 \cdot 10^7$	6.37
October	Head	47.49	4.24	3.18	8.82·10 ⁵	8.33·10 ⁵	$1.33 \cdot 10^7$	6.25
February	Head	34.08	3.81	1.97	$2.05 \cdot 10^{6}$	$2.27 \cdot 10^6$	$3.41 \cdot 10^7$	4.95
April	Head	39.67	2.07	3.61	$1.92 \cdot 10^6$	$1.68 \cdot 10^6$	$4.59 \cdot 10^7$	5.61
June	Upper	75.75	6.62	1.66	$3.36 \cdot 10^{5}$	1.72·10 ⁵	$3.84 \cdot 10^6$	6.11
August	Upper	32.53	2.82	1.46	$2.32 \cdot 10^{6}$	$2.40 \cdot 10^{6}$	$3.60 \cdot 10^7$	5.81
October	Upper	32.46	3.88	1.40	$1.92 \cdot 10^{6}$	$1.19 \cdot 10^6$	$2.52 \cdot 10^7$	5.91
February	Upper	4.05	0.65	0.11	$3.12 \cdot 10^5$	$3.17 \cdot 10^6$	$4.35 \cdot 10^6$	4.75
April	Upper	9.23	0.95	0.5	7.15·10 ⁵	$1.60 \cdot 10^6$	$1.85 \cdot 10^7$	4.67
June	Mid	60.53	2.32	9.33	$9.41 \cdot 10^4$	1.81·10 ⁵	$1.10 \cdot 10^6$	6.06
August	Mid	39.57	1.54	6.02	$2.24 \cdot 10^6$	$3.55 \cdot 10^6$	$3.39 \cdot 10^7$	5.95
October	Mid	35.52	2.70	4.25	$1.33 \cdot 10^6$	$2.11 \cdot 10^6$	$2.55 \cdot 10^7$	5.82
February	Mid	6.93	0.83	1.18	$5.51 \cdot 10^5$	9.13·10 ⁵	$6.61 \cdot 10^6$	4.71
April	Mid	29.20	2.10	3.49	$2.04 \cdot 10^{6}$	$3.64 \cdot 10^6$	$2.56 \cdot 10^7$	5.29
June	Lower	10.60	0.50	5.43	$1.84 \cdot 10^5$	$3.32 \cdot 10^5$	$1.70 \cdot 10^6$	6.09
August	Lower	3.33	0.09	3.89	$6.62 \cdot 10^5$	$2.95 \cdot 10^{6}$	$2.68 \cdot 10^7$	6.20
October	Lower	9.91	0.39	8.40	$4.93 \cdot 10^5$	$7.21 \cdot 10^6$	$1.70 \cdot 10^7$	6.42
February	Lower	1.45	0.17	2.15	$2.64 \cdot 10^5$	$7.20 \cdot 10^5$	$8.49 \cdot 10^6$	4.33
April	Lower	0.75	0.03	5.22	6.39·10 ⁵	$1.31 \cdot 10^6$	$2.18 \cdot 10^7$	5.12
June	Mouth	6.52	0.24	14.42	$6.63 \cdot 10^2$	$4.50 \cdot 10^3$	$2.13 \cdot 10^4$	4.12
August	Mouth	3.15	0.04	15.15	$7.42 \cdot 10^5$	$2.21 \cdot 10^6$	$2.06 \cdot 10^7$	6.31
October	Mouth	4.85	0.16	14.70	8.88·10 ⁵	$1.05 \cdot 10^6$	$3.10 \cdot 10^7$	6.14
February	Mouth	2.48	0.13	5.32	$5.49 \cdot 10^5$	$2.24 \cdot 10^6$	$3.37 \cdot 10^7$	4.88
April	Mouth	1.24	0.04	10.94	5.23·10 ⁵	$1.17 \cdot 10^6$	$2.62 \cdot 10^7$	5.20

DNRA rates were best predicted by the relative abundances, based on the overall 16S rRNA gene sequencing, of specific taxa carrying the nrfA gene, based on metagenomic identification. Only one multiple linear regression had a delta AICc <2 (Table S1, Supporting Information). It explained 68% of the variation

in DNRA rates and included the relative abundance of three nrfA carrying families, Anaerolineaceae (Anaerolineales), Ectothiorhodospiraceae (Gammaproteobacteria) and Prolixibacteraceae (Bacteroidales). The relative abundance of Anaerolineaceae had a negative linear relationship with DNRA rates, while relative

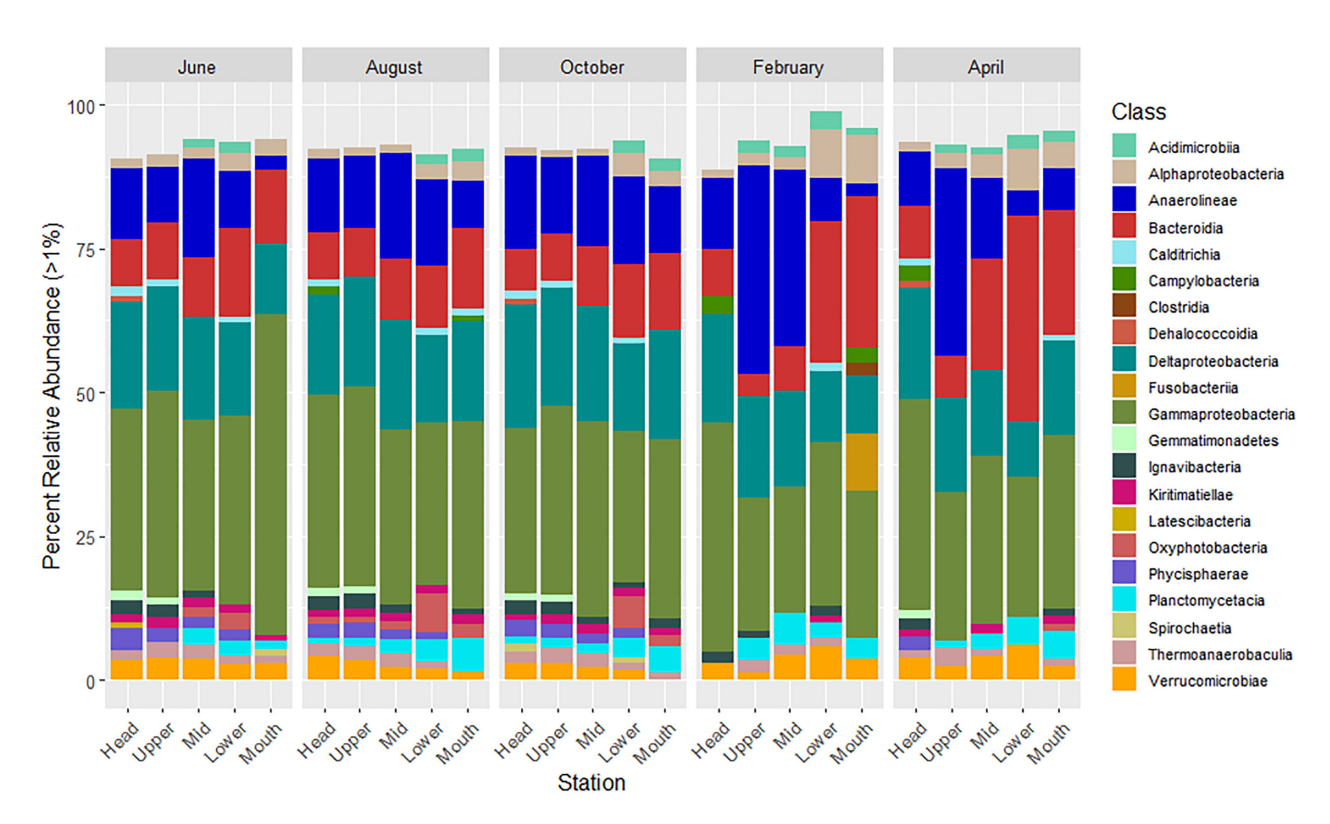


Figure 3. A stacked bar plot showing the relative abundance, greater than 1%, of classes present in each of the samples. Stations range from the head of the York River Estuary to the mouth. Samples are separated into months ranging from June 2018 to April 2019.

abundances of both Ectothiorhodospiraceae and Prolixibacteraceae had positive linear relationships (Fig. S4, Supporting Information). While no environmental characteristics were included in the top multiple linear regression, salinity, which had a positive, significant linear relationship (P < 0.05, $R^2 = 0.31$) with DNRA rates, was the best single predictor of DNRA rates in the York River. The abundance of nrfA was not a good predictor of DNRA rates in the York River. Sediment chlorophyll, based on single linear regressions that excluded June samples, had a significant positive relationship with DNRA rates (P < 0.05, $R^2 = 0.17$).

DISCUSSION

Potential denitrification rates found in the York River, especially those in the upper region of the estuary, were, for the most part, higher than rates of denitrification previously reported for other estuaries, including in the Chesapeake Bay, which ranged from 5 to 160 μ moles N m⁻² h⁻¹ (Gardner et al. 2006; Rich et al. 2008; Dong et al. 2009; Owens 2009; Giblin et al. 2010). However, rates exceeding 100 nmol N mL⁻¹ wet sediment h⁻¹ have been reported from the Thames River, UK (Trimmer, Nicholls and Deflandre 2003) (Table S2, Supporting Information). A positive relationship with water column NO_x- and a negative relationship with salinity were among the top correlations with denitrification rates in the York River, supporting past studies in which low salinity and high NO₃- concentrations have been found to increase denitrification (Kemp et al. 1990; Owens 2009; Giblin et al. 2010). Therefore, the high rates of denitrification observed in the York River were likely influenced by the above average freshwater input in June 2018, which both lowered salinity to levels not normally seen in the York River and delivered high concentrations of NO₃⁻ and organic matter. The head and upper portion of the York River are also the location of the estuarine

turbidity maximum and seasonal second turbidity maximum (Lin and Kuo 2001); rates of denitrification have been found to increase with higher suspended solids and in turbidity maximum zones in other estuaries (Abril et al. 2000; Liu et al. 2013).

Rates of anammox were higher in the York River Estuary than previously reported for the Chesapeake Bay and its tributaries (Rich et al. 2008), the New River and Cape Fear Estuaries in North Carolina, USA (Dale, Tobias and Song 2009; Lisa et al. 2014), and the Thames River, UK (Trimmer, Nicholls and Deflandre 2003) (Table S2, Supporting Information). The increase in freshwater, which delivered NO_3^- and organic C in June 2018, may have increased anammox rates in the York River, though they were still below those previously reported for the Colne River Estuary, UK, which reached 157 μ moles N m⁻² h⁻¹ (Dong et al. 2009).

This study is the first reported measurement of DNRA in the Chesapeake Bay region. York River potential DNRA rates, especially in the lower estuary, were higher than or comparable to those previously reported for estuaries in Massachusetts, USA (Giblin et al. 2010), Texas, USA (Gardner et al. 2006), North Carolina, USA (Song, Lisa and Tobias 2014) and Colne, UK (Dong et al. 2009), which ranged from 4 to just over 300 μ moles N m $^{-2}$ h $^{-1}$ (Dong et al. 2009; Giblin et al. 2010) (Table S2, Supporting Information).

Nitrate reduction in the York River Estuary was dominated by N removal through denitrification in the upper estuary, and shifted to N retention through DNRA in the lower estuary. While denitrification, and N removal in general, was higher overall, the increase in N recycling in the lower portion of the estuary increased N availability in that portion of the river and could increase the amount of $\mathrm{NH_4}^+$ exported to the Chesapeake Bay. The lower portion of the York River often experiences intense harmful algal blooms during the summer months (Marshall and Egerton 2012), which could be driven in part by an increased flux

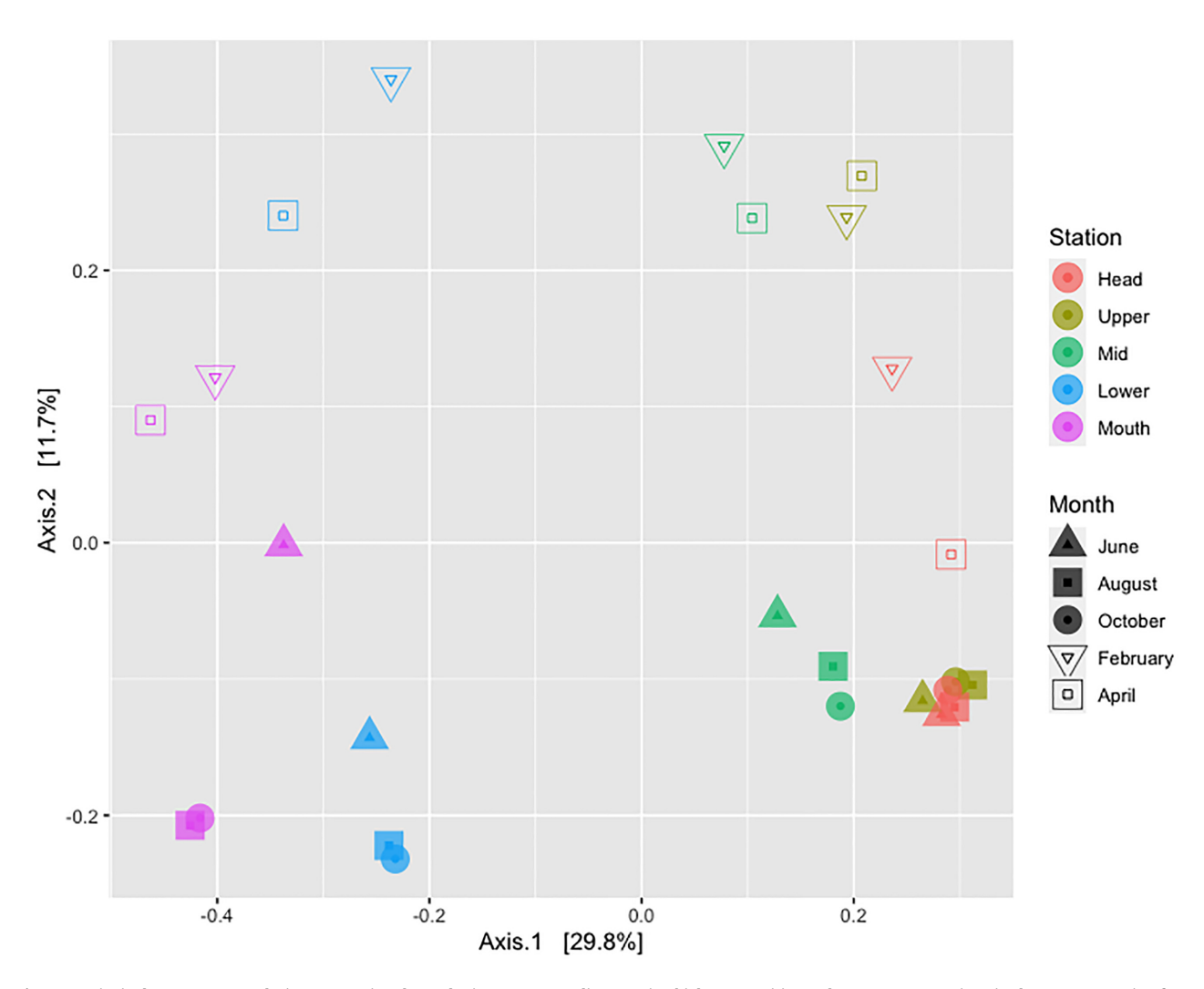


Figure 4. Principal component analysis representing the York River Estuary sediment microbial communities. Colors represent stations in the estuary ranging from the head of the estuary to the mouth. Shapes represent months from June 2018 to April 2019.

of NH₄⁺ from DNRA in lower estuarine sediments, though no harmful algal blooms took place in the lower York River during the study period. Denitrification, anammox and DNRA have previously been found to decrease from the head to the mouth of an estuary, though patterns of DNRA rates tend to be more varied (Dong et al. 2009; Lisa et al. 2014; Song, Lisa and Tobias 2014).

The shift between denitrification in the upper estuary to DNRA in the lower estuary seems to be driven by geochemical characteristics and changes in microbial communities. Sediment organic content showed a strong positive relationship with denitrification rates, and was likely the source of substrate for the denitrifying bacteria to respire. DNRA has been found to be favored when the ratio of OC to $\rm NO_3^-$ is high (Giblin et al. 2013; Hardison et al. 2015), though sediment C:N ratios showed no clear relationship with either denitrification or DNRA in this study. Denitrification was in part driven by water column nutrients; nitrogen cycling process rates are typically related directly to substrate concentrations (Kemp et al. 1990; Owens 2009), as was seen in this study with denitrification.

Environmental characteristics also play a role in influencing microbial community dynamics and beta diversity. The spatial shift in sediment community structure was linked to % sediment organic matter and water column salinity. The impact of

salinity on microbial community structure as has been found previously in temperate estuaries, including the Chesapeake Bay (Francis et al. 2013; Song, Lisa and Tobias 2014). The temporal change in beta-diversity was in part driven by temperature, a known driver of community composition in temperate estuaries. The shift in sediment microbial communities along the estuarine gradient in the same location as the switch from nitrogen removal to nitrogen retention shows the importance of understanding interactions between environmental characteristics and microbial communities and how they play a role in determining nitrogen cycling rates.

The abundances of functional genes encoding for the enzymes in N metabolic processes have been found to increase the predictive power of N cycling models, including those for denitrification and DNRA (Graham et al. 2014, 2016; Semedo and Song 2020), especially when the gene in question is carried by a small subset of bacteria (Graham et al. 2016), and have shown positive correlations with the associated process rates (Dong et al. 2009). In the York River, while denitrification activity was linked to nirS gene abundance, DNRA was not linked to nrfA gene abundance. Based on the classification of nirS genes from October microbial communities, in which Proteobacteria heavily dominated the nirS community, the nirS qPCR primer chosen for

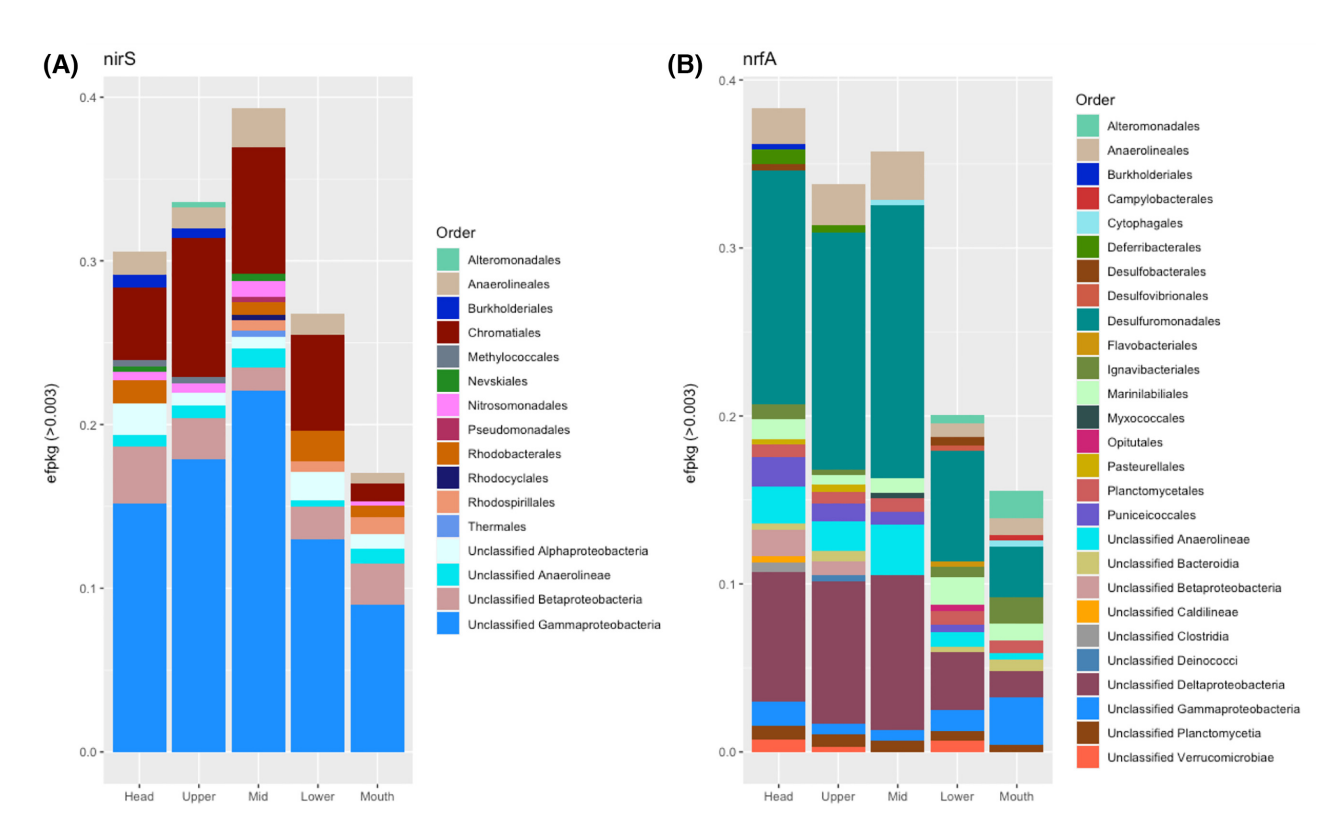


Figure 5. Normalized gene counts (efpkg) based on annotated nirS and nrfA genes from metagenomic sequencing of October York River sediment microbial communities showing the taxonomic structure of (A) denitrifying and (B) DNRA organisms.

this study likely gives an accurate representation of the quantity of nirS in the sediments. However, since nrfA genes are more diverse with a wider distribution among archaeal and bacterial lineages than nirS genes, the nrfA qPCR may not have captured all DNRA organisms. Instead of having a strong relationship to the abundance of a functional gene, DNRA was more strongly linked to the abundance of specific taxa with the capacity to perform DNRA; the relative abundances of specific groups of bacteria have been found previously to increase the predictive capabilities of models (Graham et al. 2016; Semedo and Song 2020).

Many microbial taxa can perform similar functions, and not all microbes capable of performing a specific function always utilize that pathway. This makes understanding which of the many microbial taxa in complex microbial assemblages is contributing to a specific community function challenging. In this study we observed a clear spatial shift in beta diversity between the upper and lower estuary that corresponded with a shift from NO₃⁻ removal, largely in the form of denitrification, to NO₃⁻ retention through DNRA. To better understand the shifts in taxa that were driving the shift in NO₃- reduction processes, especially since nrfA gene abundances were not good predictors of DNRA rates, we performed metagenomic sequencing on a subset of the samples and identified specific taxa carrying the nrfA gene. With that data set, we were able to identify which taxa in the microbial community were capable of performing DNRA, and determine which of those specific taxa, based on their overall relative abundance in the 16S rRNA gene sequences, were good predictors of DNRA rates.

The lack of a relationship between DNRA rates and nrfA gene abundance suggests that DNRA activity was largely driven by

only a few bacterial families; due to the strong positive relationships between DNRA rates and Ectothiorhidospiraceae and Prolixibacteraceae, it is likely these families were primarily responsible for DNRA. On the other hand, the abundance of nirS was among the top predictors for denitrification implying that in the York River, denitrification activity was driven and performed by a large group of denitrifying microbes rather than individual taxa. This disparity between the microbial drivers of denitrification and DNRA could be due to the physiology of the taxa involved in these processes. Denitrifying microbes are most commonly capable of using only oxygen or NO₃⁻ in their metabolism while DNRA bacteria have a variety of energy metabolism options including fermentation, sulfate reduction, denitrification and anammox in addition to DNRA (Giblin et al. 2013; Helen et al. 2016). Therefore, the nirS carrying microbes were likely to be performing denitrification in the estuarine sediments, leading to the strong relationship observed between nirS gene abundance and denitrification, while the nrfA carrying microbes could have been performing a number of different processes with only certain taxa, actively performing DNRA. This is further supported by the negative relationship between the relative abundance of Anaerolineaceae and DNRA rates, which implies that, though Anaerolineaceae is genetically capable of performing DNRA, these organisms were utilizing an alternative metabolic pathway and not contributing to the observed rates of DNRA.

Understanding variation in N removal and retention across estuaries is important to determine the availability of N for use by primary producers. The competition between denitrification and DNRA has previously been found to vary seasonally (Kelly-Gerreyn, Trimmer and Hydes 2001) and be controlled

along estuaries by environmental characteristics (Gardner et al. 2006; Giblin et al. 2010, 2013; Song, Lisa and Tobias 2014; Hardison et al. 2015). The shift from denitrification in the upper estuary to DNRA in the lower estuary that is persistent throughout all seasons observed in this study is different from previously reported patterns. The dominance of DNRA in the lower estuary increases the amount of bioavailable N in the lower portion of the York River system, possibly supporting the seasonal harmful algal blooms and subsequent hypoxia in bottom water that occur in the lower estuary most years (Reay 2009; Marshall and Egerton 2012). Understanding the switch in dominant NO₃reduction pathways requires an understanding of the impacts of environmental gradients, as well as shifts in microbial community structure that exist in an estuarine system. In the York River, changes in sediment organic matter and water column nutrient concentrations were strongly linked to denitrification. The York River sediment microbial community experiences a large shift in community structure at the same location that DNRA begins to outcompete denitrification for available nitrate. This shift, which is linked to the overall nirS carrying microbial community and specific taxa capable of performing DNRA, is an important regulatory aspect that is often ignored in studies examining N cycling in ecosystems.

ACKNOWLEDGMENTS

The authors would like to thank Hunter Walker, Stephanie Wilson, Michelle Woods, Derek Detweiler, Kimberly Reece, Mark Brush, Michele Cochran and Renia Passie for assistance in the lab and field.

SUPPLEMENTARY DATA

Supplementary data are available at FEMSEC online.

FUNDING

Funding for this work was provided by the National Science Foundation (OCE 1737258).

Conflict of interest. None declared.

REFERENCES

- Abril G, Riou SA, Etcheber H et al. Transient, tidal time-scale, nitrogen transformations in an estuarine turbidity maximum: fluid mud system (the Gironde, South-West France). Estuarine Coastal Shelf Sci 2000;50:703–15.
- Andrews S. FastQC: a quality control tool for high throughput sequence data. 2010. https://github.com/s-andrews/FastQC#:~:text=FastQC%20is%20a%20program%20designed,report%20which%20summarises%20the%20results.
- Arkin AP, Cottingham RW, Henry CS et al. KBase: the United States Department of Energy Systems Biology Knowledgebase. Nat Biotechnol 2018;36:566–9.
- Barton K. Mu-MIn: multi-model inference. 2009. https://CRAN.R-project.org/package=MuMIn.
- Bohlen L, Dale AW, Sommer S et al. Benthic nitrogen cycling traversing the Peruvian oxygen minimum zone. *Geochim Cosmochim Acta* 2011;75:6094–111.
- Bolger AM, Lohse M, Usadel B. Trimmomatic: a flexible trimmer for Illumina sequence data. Bioinformatics 2014;30:2114–20.

- Callahan BJ, McMurdie PJ, Rosen MJ et al. DADA2: high-resolution sample inference from Illumina amplicon data. Nat Methods 2016;13:581–3.
- Caporaso JG, Lauber CL, Walters WA et al. Global patterns of 16S rRNA diversity at a depth of millions of sequences per sample. Proc Natl Acad Sci USA 2011;108:4516–22.
- Dale OR, Tobias CR, Song B. Biogeographical distribution of diverse anaerobic ammonium oxidizing (anammox) bacteria in Cape Fear River Estuary. *Environ Microbiol* 2009;11:1194–207.
- Dong LF, Smith CJ, Papaspyrou S et al. Changes in benthic denitrification, nitrate ammonification, and anammox process rates and nitrate and nitrite reductase gene abundances along an estuarine nutrient gradient (the Colne Estuary, United Kingdom). Appl Environ Microbiol 2009;75:3171–9.
- Francis CA, O'Mullan GD, Cornwell JC et al. Transitions in nirStype denitrifier diversity, community composition, and biogeochemical activity along the Chesapeake Bay estuary. Front Microbiol 2013;4:1–12.
- Gardner WS, McCarthy MJ, An S et al. Nitrogen fixation and dissimilatory nitrate reduction to ammonium (DNRA) support nitrogen dynamics in Texas estuaries. Limnol Oceanogr 2006;51:558–68.
- Giblin A, Tobias C, Song B et al. The importance of dissimilatory nitrate reduction to ammonium (DNRA) in the nitrogen cycle of coastal ecosystems. *Oceanography* 2013;26:124–31.
- Giblin AE, Weston NB, Banta GT et al. The effects of salinity on nitrogen losses from an oligohaline estuarine sediment. Estuaries Coast 2010;33:1054–68.
- Graham EB, Knelman JE, Schindlbacher A et al. Microbes as engines of ecosystem function: when does community structure enhance predictions of ecosystem processes? Front Microbiol 2016;7:214.
- Graham EB, Wieder WR, Leff JW et al. Do we need to understand microbial communities to predict ecosystem function? A comparison of statistical models of nitrogen cycling processes. Soil Biol Biochem 2014;68:279–82.
- Hardison AK, Algar CK, Giblin AE et al. Influence of organic carbon and nitrate loading on partitioning between dissimilatory nitrate reduction to ammonium (DNRA) and n_2 production. Geochim Cosmochim Acta 2015;164:146–60.
- Helen D, Kim H, Tytgat B et al. Highly diverse nirK genes comprise two major clades that harbour ammonium-producing denitrifiers. BMC Genomics 2016;17:1–13.
- Kandeler E, Deiglmayr K, Tscherko D et al. Abundance of narG, nirS, nirK, and nosZ genes of denitrifying bacteria during primary successions of a glacier foreland. Appl Environ Microbiol 2006;72:5957–62.
- Kelly-Gerreyn BA, Trimmer M, Hydes DJ. A diagenetic model discriminating denitrification and dissimilatory nitrate reduction to ammonium in a temperate estuarine sediment. Mar Ecol Prog Ser 2001;220:33–46.
- Kemp WM, Boynton WR, Adolf JE et al. Eutrophication of Chesapeake Bay: historical trends and ecological interactions. Mar Ecol Prog Ser 2005;303:1–29.
- Kemp WM, Sampou P, Caffrey J et al. Ammonium recycling versus denitrification in Chesapeake Bay sediments. Limnol Oceanogr 1990;35:1545–63.
- Lin J, Kuo AY. Secondary turbidity maximum in a partially mixed microtidal estuary. Estuaries 2001;24:707–20.
- Lisa JA, Song B, Tobias CR et al. Impacts of freshwater flushing on anammox community structure and activities in the New River Estuary, USA. Aquat Microb Ecol 2014;72:17–31.

- Liu T, Xia X, Liu S et al. Acceleration of denitrification in turbid rivers due to denitrification occurring on suspended sediment in oxic waters. Environ Sci Technol 2013;47:4053-61.
- Marshall HG, Egerton TA. Bloom and toxin producing algae in Virginia tidal rivers. Ocean 2012 MTS/IEEE Harnessing Power Ocean 2012. DOI: 10.1109/OCEANS.2012.6404820.
- McMurdie PJ, Holmes S. Phyloseq: an R package for reproducible interactive analysis and graphics of microbiome census data. PLoS One 2013;8. DOI: 10.1371/journal.pone.0061217.
- Mohan SB, Schmid M, Jetten M et al. Detection and widespread distribution of the nrfA gene encoding nitrite reduction to ammonia, a short circuit in the biological nitrogen cycle that competes with denitrification. FEMS Microbiol Ecol 2004:49:433-43.
- Oksanen J, Blanchet FG, Friendly M et al. vegan: community ecology package. 2018. https://CRAN.R-project.org/package=veg
- Owens M. Nitrogen cycling and controls on denitrification in mesohaline sediments of Chesapeake Bay. Master of Science Thesis. Faculty of the Graduate School of the University of Maryland, College Park. 2009.
- Parada AE, Needham DM, Fuhrman JA. Every base matters: assessing small subunit rRNA primers for marine microbiomes with mock communities, time series and global field samples. Environ Microbiol 2016;18:1403-14.
- R Core Team. R: a language and environment for statistical computing. 2018. https://www.r-project.org/.
- Reay WG. Water quality within the York River Estuary. J Coast Res 2009;10057:23-39.
- Rich JJ, Dale OR, Song B et al. Anaerobic ammonium oxidation (anammox) in Chesapeake Bay sediments. Microb Ecol 2008;55:311-20.
- Risgaard-Petersen N, Rysgaard S. Nitrate reduction in sediments and waterlogged soil measured by 15N techniques. Methods Appl Soil Microbiol Biogeochem 1995:287-95.

- Salk KR. Erler DV. Evre BD et al. Unexpectedly high degree of anammox and DNRA in seagrass sediments: description and application of a revised isotope pairing technique. Geochim Cosmochim Acta 2017;211:64-78.
- Schultz GE, Ducklow H. Changes in bacterioplankton metabolic capabilities along a salinity gradient in the York River estuary, Virginia, USA. Aquat Microb Ecol 2000;22: 163-74.
- Semedo M, Song B. From genes to nitrogen removal: determining the impacts of poultry industry wastewater on tidal creek denitrification. Environ Sci Technol 2020;54:146-57.
- Song B, Lisa JA, Tobias CR. Linking DNRA community structure and activity in a shallow lagoonal estuarine system. Front Microbiol 2014;5:1-10.
- Song B, Tobias CR. Molecular and stable isotope methods to detect and measure anaerobic ammonium oxidation (anammox) in aquatic ecosystems. Methods Enzymol 2011;496: 63-89
- Trimmer M, Nicholls JC, Deflandre B. Anaerobic ammonium oxidation measured in sediments along the Thames Estuary, United Kingdom. Appl Environ Microbiol 2003;69: 6447-54.
- Welsh A, Chee-Sanford JC, Connor LM et al. Refined NrfA phylogeny improves PCR-based nrfA gene detection. Appl Environ Microbiol 2014;80:2110-9.
- Wickham H. ggplot2: create elegant data visualisations using the grammar of graphics. 2005. https://cran.r-project.org/web/p ackages/ggplot2/index.html.
- Yilmaz P, Parfrey LW, Yarza P et al. The SILVA and "all-species Living Tree Project (LTP)" taxonomic frameworks. Nucleic Acids Res 2014;42:643-8.
- Yin G, Hou L, Liu M et al. A novel membrane inlet mass spectrometer method to measure 15NH4+ for isotopeenrichment experiments in aquatic ecosystems. Environ Sci Technol 2014;48:9555-62.